

Attenuation of Simian Immunodeficiency Virus SIVmac239 Infection by Prophylactic Immunization with DNA and Recombinant Adenoviral Vaccine Vectors Expressing Gag

Danilo R. Casimiro,^{1*} Fubao Wang,¹ William A. Schleif,¹ Xiaoping Liang,¹ Zhi-Qiang Zhang,¹ Timothy W. Tobery,¹ Mary-Ellen Davies,¹ Adrian B. McDermott,¹ David H. O'Connor,³ Arthur Fridman,² Ansu Bagchi,² Lynda G. Tussey,¹ Andrew J. Bett,¹ Adam C. Finnefrock,¹ Tong-ming Fu,¹ Aimin Tang,¹ Keith A. Wilson,¹ Minchun Chen,¹ Helen C. Perry,¹ Gwendolyn J. Heidecker,¹ Daniel C. Freed,¹ Anthony Carella,¹ Kara S. Punt,¹ Kara J. Sykes,¹ Lingyi Huang,¹ Virginia I. Ausensi,¹ Margaret Bachinsky,¹ Usha Sadasivan-Nair,¹ David I. Watkins,³ Emilio A. Emini,¹ and John W. Shiver¹

Department of Vaccines and Biologics Research, Merck Research Laboratories, Merck & Co., West Point, Pennsylvania 19486¹; Applied Computer Sciences and Mathematics, Merck Research Laboratories, Merck & Co., Rahway, New Jersey 07065²; and Department of Pathology and Laboratory Medicine, University of Wisconsin, Madison, Wisconsin³

Received 14 April 2005/Accepted 7 August 2005

The prophylactic efficacy of DNA and replication-incompetent adenovirus serotype 5 (Ad5) vaccine vectors expressing simian immunodeficiency virus (SIV) Gag was examined in rhesus macaques using an SIVmac239 challenge. Cohorts of either Mamu-A*01(+) or Mamu-A*01(-) macaques were immunized with a DNA prime-Ad5 boost regimen; for comparison, a third cohort consisting of Mamu-A*01(+) monkeys was immunized using the Ad5 vector alone for both prime and boost. All animals, along with unvaccinated control cohorts of Mamu-A*01(+) and Mamu-A*01(-) macaques, were challenged intrarectally with SIVmac239. Viral loads were measured in both peripheral and lymphoid compartments. Only the DNA prime-Ad5-boosted Mamu-A*01(+) cohort exhibited a notable reduction in peak plasma viral load (sevenfold) as well as in early set-point viral burdens in both plasma and lymphoid tissues (10-fold) relative to those observed in the control monkeys sharing the same Mamu-A*01 allele. The degree of control in each animal correlated with the levels of Gag-specific immunity before virus challenge. However, virus control was short-lived, and indications of viral escape were evident as early as 6 months postinfection. The implications of these results in vaccine design and clinical testing are discussed.

There is increasing evidence that anti-human immunodeficiency virus type 1 (HIV-1) cellular immunity, particularly that associated with CD8⁺ T cells, plays a prominent role in controlling viral infection and progression to disease (2, 14, 17, 25, 28). In recent years, several vaccine vector approaches capable of eliciting this type of immune response have been developed (5, 6, 8, 10, 28, 33). Central to the evaluation of such vaccine vectors is the ability to assess their potency in nonhuman primates against challenges with simian immunodeficiency viruses (SIV). Virus strains used in such studies include, among others, SIVmac239 (1, 32), SIVsmE660 (7, 23, 27), SIVmac251 (11, 23), and hybrid viruses such as simian-human immunodeficiency virus SHIV89.6P (2, 3, 26, 28). These viruses exhibit different pathogenic properties which may or may not approximate the course of HIV-1 infection in humans. Hence, it is important to test candidate vaccines against more than one of the simian viruses in order to fully appreciate the potential of any given immunization approach.

We compared the efficacy in monkeys of a DNA vector and of two viral vaccine vectors, modified vaccinia Ankara and

replication-defective adenovirus serotype 5 (Ad5), expressing an SIV Gag protein to attenuate SHIV89.6P infection following challenge (28). The Ad5 vector, used either alone or in combination with DNA priming, proved to be highly immunogenic and effective in mitigating the virus challenge. In the current report, we extend our evaluation by immunizing rhesus macaques using the same Ad5-based approaches and assessing the effect of the resulting immune response against challenge with the SIVmac239 virus. Further analyses of the breadth of the immune responses and their relationship with virus diversity are discussed in an accompanying article (18).

MATERIALS AND METHODS

Vaccines. A gene coding for SIVmac239 Gag was synthesized based on codons frequently used in mammalian cells (28). The gene was subcloned into the expression vector V1Jns, placing it under the control of the human cytomegalovirus (hCMV) promoter with intron A and a bovine growth hormone polyadenylation sequence (29). Solutions (5 mg/ml) of this V1Jns/SIV gag construct were formulated with 7.5 mg/ml of a nonionic block copolymer, CRL1005 (CytRx Corp., Atlanta, GA), and 0.85 mM of a cationic detergent, benzalkonium chloride (Ruger Chemical Co., Irvington, NJ). A replication-defective E1-, E3-deleted Ad5 vector expressing the same SIVmac239 gag gene (Ad5/SIV gag) was constructed following previously established procedures (28).

Immunization and SIV infection. Indian rhesus macaques (*Macaca mulatta*) were typed for Mamu-A*01 allele expression using established PCR methods (16). Cohorts of 5 Mamu-A*01(+) animals were immunized either three times with 10¹¹ viral particles (vp) of Ad5/SIV gag (at weeks 0, 4, and 24) or three times with 5 mg of V1Jns/SIV gag formulated in the CRL1005/BAK adjuvant (weeks

* Corresponding author. Mailing address: Department of Vaccines and Biologics Research, Merck Research Laboratories, Merck & Co., West Point, Pennsylvania 19486. Phone: (215) 652-3129. Fax: (215) 652-7320. E-mail: danilo_casimiro@merck.com.

0, 4, and 8) and followed by a single 10^{11} -vp Ad5/SIV gag booster shot (at week 24). A third cohort consisting of 5 Mamu-A*01(-) monkeys received the same heterologous DNA prime-Ad5 boost regimen. In all cases, the total vaccine dose was suspended in 1 ml of buffered solution. The macaques were anesthetized (ketamine-xylazine), and the vaccines were delivered intramuscularly in 0.5-ml aliquots into both deltoid muscles with tuberculin syringes (Becton-Dickinson, Franklin Lakes, N.J.). Plasma and peripheral blood mononuclear cell (PBMC) samples were collected following standard protocols.

The SIVmac239 nef/open virus stock used in this study was graciously provided by Ronald Desrosiers (Harvard Medical School, Southborough, MA). Each vaccinated animal received 1×10^4 50% tissue culture infectious doses of the virus intrarectally. Nonvaccine cohorts consisting of either 5 Mamu-A*01(+) or 5 Mamu-A*01(-) macaques were likewise infected with the same virus dose. All animal care and treatment were in accordance with standards approved by the Institutional Animal Care and Use Committee according to the principles set forth in the Guide for Care and Use of Laboratory Animals, Institute of Laboratory Animal Resources, National Research Council.

ELISPOT and ICS assays. Ninety-six-well flat-bottomed plates (Immobilon-P membrane; Millipore) were coated with $1 \mu\text{g}/\text{well}$ of anti-gamma interferon (IFN- γ) monoclonal antibody MD-1 (U-Cytech-BV) overnight at 4°C . The plates were then washed three times with phosphate-buffered saline (PBS) and were blocked with R10 medium (RPMI, 0.05 mM 2-mercaptoethanol, 1 mM sodium pyruvate, 2 mM L-glutamate, 10 mM HEPES, 10% fetal bovine serum) for 2 h at 37°C . The medium was discarded from the plates, and freshly isolated peripheral blood mononuclear cells (PBMCs) were added at 1×10^5 to 4×10^5 cells/well. The cells were stimulated in the absence (mock) or presence of defined peptide or peptide pools (4 $\mu\text{g}/\text{ml}$ per peptide). Pools consisting of 20-amino-acid (aa) peptides shifting by 10 aa (Synpep) were constructed from entire SIVmac239 Gag, Pol, gp140, or Tat sequences. An SIVmac239 peptide pool was constructed from 15-aa peptide shifting by 11 aa. The Gag₁₈₁₋₁₈₉ CM9 peptide was likewise synthesized. Cells were then incubated for 20 to 24 h at 37°C in 5% CO_2 . Plates were washed six times with PBST (PBS, 0.05% Tween 20), 100 $\mu\text{l}/\text{well}$ of a 1:400 dilution of anti-IFN- γ polyclonal biotinylated detector antibody solution (U-Cytech-BV) was added, and the plates were incubated overnight at 37°C . The plates were washed six times with PBST. Color was developed by incubating in nitroblue tetrazolium-5-bromo-4-chloro-3-indolylphosphate (Pierce) for 10 min. Spots were counted under a dissecting microscope and normalized to 1×10^6 PBMC. Intracellular staining for IFN- γ production (ICS) was conducted following a previously established protocol (6).

Tetramer staining and memory phenotyping. Whole blood was collected by venous puncture into EDTA tubes and transported overnight at ambient temperature. One-hundred microliters of anticoagulant-treated blood was transferred to each of two 12- by 75-mm polystyrene fluorescence-activated cell sorter (FACS) tubes. To each tube, 0.1 μl (10 μl of a 1:100 dilution in PBS) of a pretitrated stock of the Mamu-A*01 Gag tetramer, CM9 (custom synthesis), was added. The mixtures were incubated for 20 min in the dark at room temperature. To one tube, 60 μl of cocktail containing pretitrated amounts of anti-CD8-peridinin-chlorophyll-protein complex (PerCP), anti-CD45RA-fluorescein isothiocyanate, and anti-CD27-allophycocyanin (all from Becton Dickinson) was added. To the other tube, 60 μl of cocktail containing pretitrated amounts of anti-CD8-PerCP, anti-CD45RA-fluorescein isothiocyanate, and anti-CD28-allophycocyanin (all from Becton Dickinson) was added. Tubes were incubated for an additional 20 min in the dark at room temperature. For red blood cell lysis, 1 ml/tube of $1 \times$ FACS lyse (Becton Dickinson) was added, and the tube was incubated for 10 min in the dark at room temperature. FACS wash buffer (2.5 ml; PBS plus 5% fetal calf serum plus 0.01% sodium azide) was added to each tube, and the cells were pelleted at $250 \times g$ for 10 min. Cells were resuspended in 300 μl of 1% formaldehyde and analyzed using a FACSCalibur flow cytometer (Becton Dickinson). Following acquisition, we analyzed flow cytometry data using Cell Quest software. Samples are gated on the CD8 $^+$ lymphocyte population for tetramer analysis and on the tetramer-positive CD8 $^+$ lymphocytes for phenotyping analysis. Phenotypes are defined as described earlier (31).

Plasma VL and CD4 quantitation. Plasma viral load (VL) was measured by a modified version of the ROCHE AMPLICOR UltraSensitive Assay, referred to as the SIV UltraSensitive Real-Time PCR Assay, with a quantification limit of 50 viral RNA copies/ml. Circulating CD4 levels were determined using Becton Dickinson TruCount tubes.

Neutralizing antibody assay. Viral neutralization assays were conducted using methods previously published (20). Briefly, CEMX174 human T-lymphoid cells were infected with SIVmac239 at a multiplicity of infection of ~ 0.01 , incubated overnight, and then washed extensively and plated onto 96-well plates. Test sera were diluted by twofold serial dilutions and mixed with the cells. Cultures were incubated an additional 72 h and then assayed for viral production by a com-

mercial SIV viral core p27 assay kit (Coulter Immunology). Endpoint titers were recorded as the reciprocal of the serum dilution in which 90% or more of the viral antigen production was inhibited compared to that in untreated viral growth control wells.

In situ hybridization (ISH) of viral RNA and viral load quantification in lymph nodes (LNs). Sequential LN biopsies (inguinal and axillary LNs) were performed on all monkeys at 45 and 190 days after virus challenge. LN tissues were collected and fixed in 4% paraformaldehyde and Molecular Biology Fixative (Streck Laboratories, Omaha, NE). Viral RNA was detected by ISH with ^{35}S -labeled RNA probes as described previously (35).

The frequencies of SIV RNA(+) cells and follicular dendritic cell (FDC)-associated viral load were determined in a representative section by quantitative image analysis of autoradiographs illuminated by epipolarized light (35). To reconstruct the entire tissue section, multipanel digital images (final magnification, $\times 160$) were captured by using an Olympus microscope (BX51) fitted with a motorized stage (Prior, Rockland, MA) and an RT Spot digital camera (Diagnostic Instruments, Inc., Sterling Heights, MI). MetaMorph software (Universal Imaging, West Chester, PA) was then used to measure the frequency of SIV RNA(+) cells and the silver grains in germinal center which were distinguished from background. The frequency of cells with viral RNA (vRNA) in a defined tissue area (in square millimeters) was determined with the calibration tool. Viral RNA on the FDC network was determined as the silver grain counts of vRNA per germinal center (also in square millimeters).

Statistical analysis. Comparisons of cohort immune or virological parameters were performed by calculating the ratios of the cohort geometric means (GM) and the associated 95% confidence intervals (95% CI); confidence intervals not overlapping with unity suggest a statistically significant difference. Correlates of disease protection were determined by associating prechallenge predictor variables and postchallenge VL values. Spearman's Rho, a nonparametric and robust rank-based statistical test (12), was used to detect trends of monotonic relationships between VL data and these predictor candidates. Data analyses were carried out using JMP 5.0.1 software (SAS Institute, Cary, NC).

RESULTS

Vaccine-elicited immunity. Cohorts of five Mamu-A*01(+) animals were immunized with either three doses of Ad5/SIV gag (weeks 0, 4, and 24) (Ad5/Ad5 cohort) or two priming doses of V1Jns/SIV gag (weeks 0, 4, and 8) followed by a booster Ad5/SIV gag dose (week 24) (DNA/Ad5 cohort). A third cohort consisting of five Mamu-A*01(-) monkeys received the same DNA prime-Ad5 boost regimen. Gag-specific T cells in peripheral blood samples were measured by IFN- γ ELISPOT and ICS, using Gag peptide pools and a defined peptide representing the Mamu-A*01-restricted CD8 epitope CM9. Immune responses to this epitope were also quantitated by tetramer staining. Priming immunizations with Ad5/SIV gag resulted in levels of CM9-specific T lymphocytes (GM of 1.3% of CD8 $^+$ CD3 $^+$ cells) that were 5.9-fold (95% CI of 2.3 to 15) higher than those elicited by the DNA immunizations (GM of 0.2%) (Fig. 1). This result paralleled the relative ELISPOT responses against the full Gag peptide pool (Fig. 2). For the Mamu-A*01(+) monkeys, the immune responses were substantially diminished (average n -fold reduction of 3.0 [95% CI of 1.9 to 5.0] at week 12) when the CM9-bearing peptide was excluded from the peptide pool used for stimulation (Fig. 2A). This suggested that the responses were directed largely to the CM9 epitope. No such reduction in ELISPOT responses with CM9 exclusion was observed in Mamu-A*01(-) monkeys (Fig. 2B).

Administration of the Ad5/SIV gag booster in Mamu-A*01(+) animals primed with the DNA vaccine elicited CM9-specific T-cell responses (GM of 5.1% of CD3 $^+$ CD8 $^+$ cells at week 26) that were 2.5-fold (95% CI of 1.2- to 5.1-fold) higher than those in Ad5-primed animals (2.1%) (Fig. 1). The post-boost immune responses in the latter cohort were not signifi-

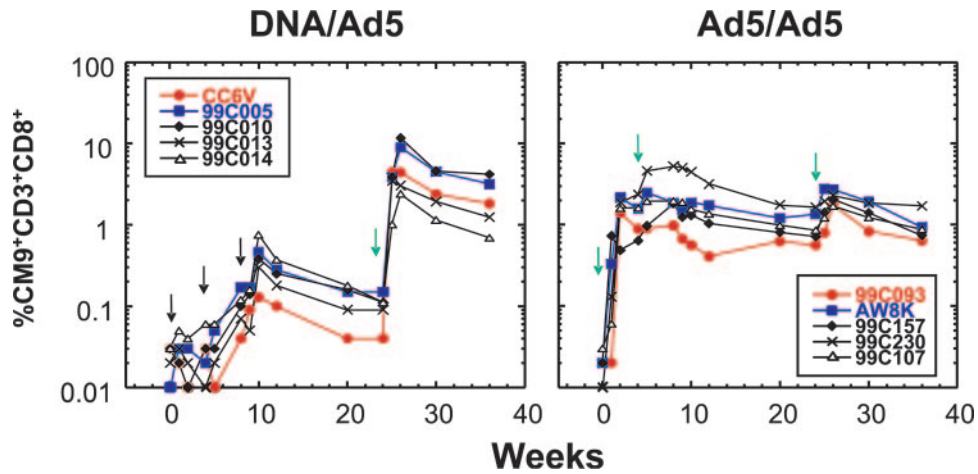


FIG. 1. Percentages of circulating CD3⁺ CD8⁺ T lymphocytes that stained positively with the Gag CM9 tetramer. Values are shown for individual animals (identity numbers are in the inset boxes) during the course of immunization. The times of immunization are indicated (black and green arrows for DNA and Ad5 vaccines, respectively).

cantly better than the peak postprime responses, presumably due to anti-vector immunity induced by the initial two Ad5 doses. The levels of anti-Gag T cells as measured by IFN- γ ELISPOT against the full peptide pool (Fig. 2) were comparable for both Mamu-A*01(-) and Mamu-A*01(+) DNA/Ad5 vaccinees (at week 28, GM of 1,008 versus 1,328 spot-forming cells (SFC)/10⁶ PBMC, respectively). While the levels at week 36 dropped faster for the Mamu-A*01(-) DNA/Ad5 vaccinees than those of the Mamu-A*01(+) DNA/Ad5 animals (GM of 479 versus 1,142 SFC/10⁶ PBMC, respectively) from the peak levels, the intercohort difference remained statistically insignificant. Consistent with previous findings, characterization of the postboost Gag-specific T-cell population by IFN- γ ICS demonstrated CD8⁺-biased responses for both immunization regimens.

The phenotypes of the CM9-specific T cells were also examined by monitoring the expression of CD45RA, CD27, and CD28 on the tetramer-positive T cells and were defined according to the model described previously (31). At the time of boost, the CM9-positive T cells in the Ad5-primed Mamu-A*01(+) macaques were largely of the acute (CD45RA⁻ CD27⁺ CD28⁻) (cohort mean of 34% of the CM9-positive T cells) mixed with the memory (CD45RA⁻ CD27⁺ CD28⁺) phenotype (mean of 16% of the CM9-positive T cells); similar analyses of the DNA-primed animals were not possible, because the levels of CM9-positive T cells were <0.2% of CD3⁺ CD8⁺ cells. After boosting, the distribution shifted, as anticipated, towards the acute expansion phenotype, which remained the predominant population up to the time of challenge (mean of 71% for DNA/Ad5 and 40% of the

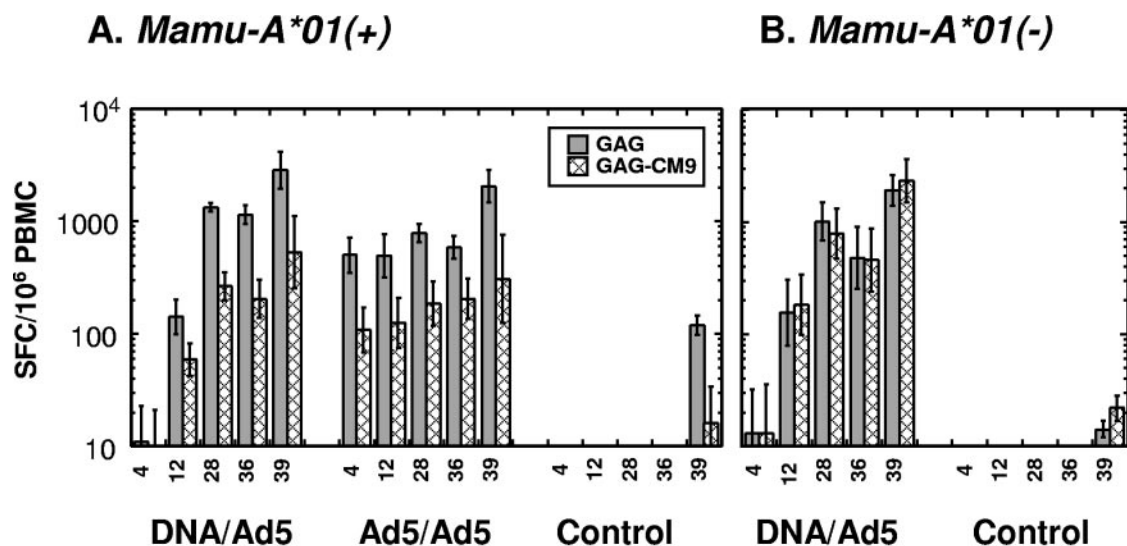


FIG. 2. Levels of Gag-specific T lymphocytes for all Mamu-A*01(+) and Mamu-A*01(-) cohorts (as measured by ELISPOT assay against the complete Gag pool [Gag] or a pool excluding the CM9-bearing peptides [Gag-CM9]) as a function of the number of weeks after start of the immunization. The cohort geometric means of the mock-subtracted SFC/10⁶ PBMC values are shown. The standard errors of the geometric means are indicated. Week 39 represents 3 weeks postinfection.

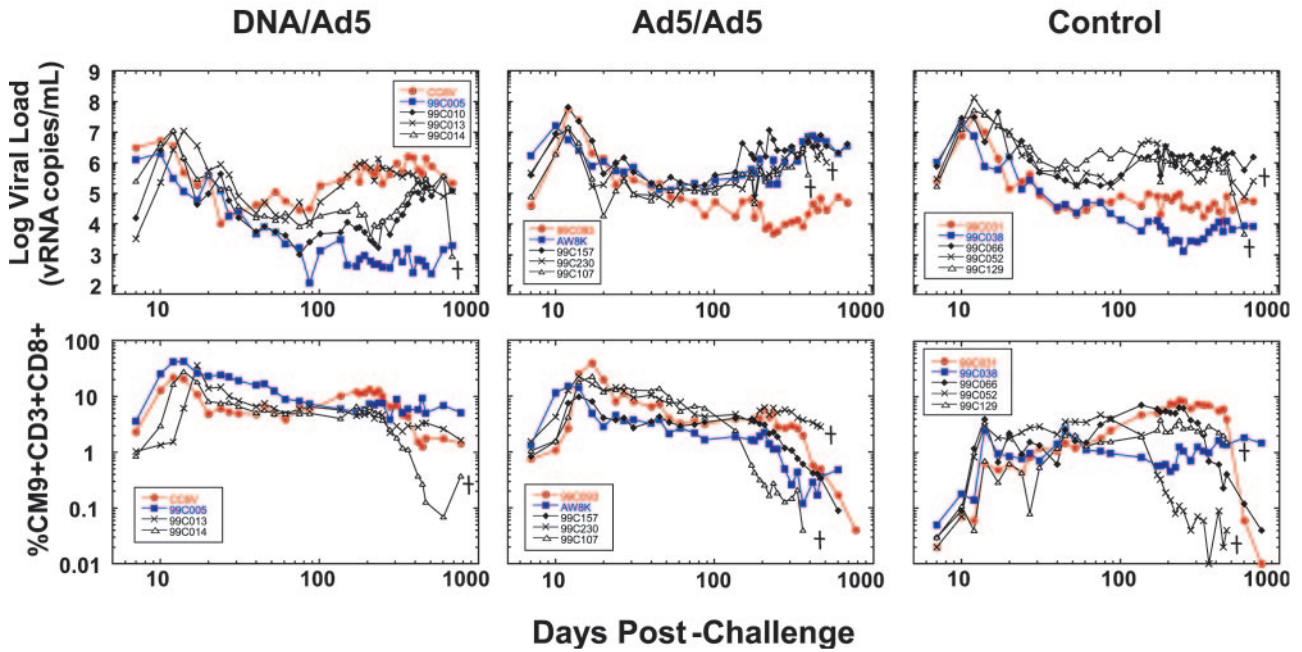


FIG. 3. Plasma viral loads and CM9(+) cell levels in Mamu-A*01(+) vaccinated and control groups following intrarectal challenge with SIVmac239.

CM9-positive T cells for Ad5/Ad5). At the time of challenge, terminally differentiated effector cells (CD45RA⁺ CD27⁻ CD28⁻) accounted for 0.6 to 9% of the CM9-positive T cells in all the animals tested.

Viremia following SIVmac239 infection. Infection with SIVmac239 resulted in vigorous viral replication, peaking at either day 12 or 14 for most animals (Fig. 3 and 4). Monkeys immunized with the DNA/Ad5 regimen exhibited an attenuation of the peak viral replication. The cohort geometric mean of the peak viral loads (VL) for the DNA/Ad5 Mamu-A*01(+) group (GM of 6.7×10^6 copies/ml) was 6.7-fold lower (95% CI of 2.2 to 20) than that of the nonvaccine Mamu-A*01(+) control (4.5×10^7 copies/ml). The geometric mean peak VL

was about 3.2-fold lower for the DNA/Ad5 Mamu-A*01(-) cohort relative to that of the Mamu-A*01(-) control group (1.4 versus 4.4×10^7 copies/ml, respectively), but this difference was not significant at the 95% confidence level. No apparent attenuation of the peak VL relative to the nonvaccine control was observed for the Ad5/Ad5 Mamu-A*01(+) cohort (GM of 2.6×10^7 copies/ml; 95% CI of the control/vaccine ratio of 0.6 to 5.3).

The postacute phase of SIVmac239 infection in several animals was characterized by an initial plateau in VLs during the second to third month (set-point phase) followed by a rebound event starting in the fourth month (chronic phase). The peak VLs determined the early set-point levels. The cohort geometric

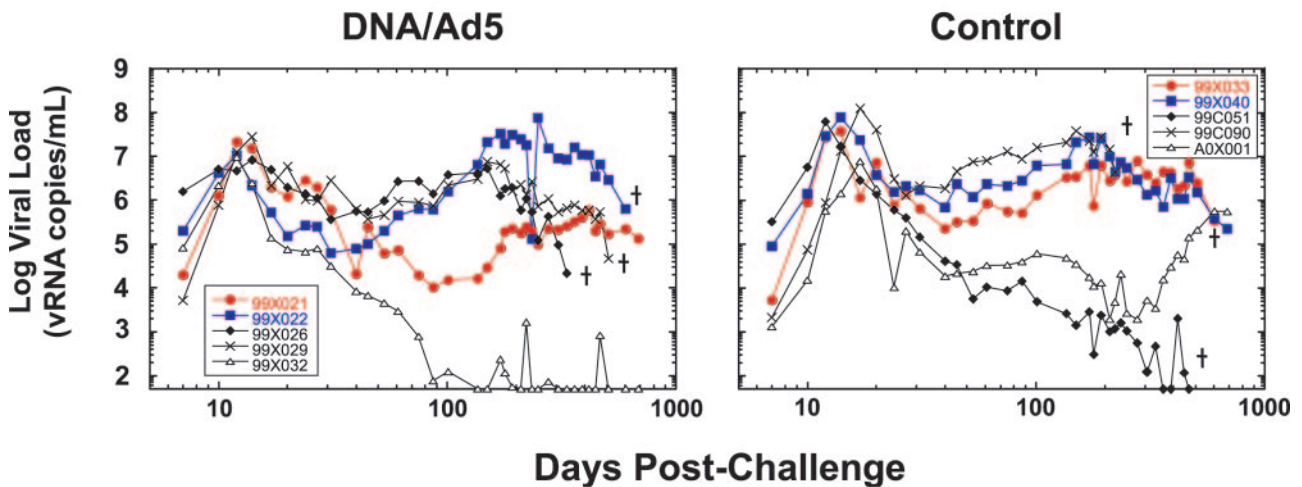


FIG. 4. Plasma viral loads in Mamu-A*01(-) vaccinated and control groups following SIVmac239 infection.

mean of set-point VL levels (each taken as the geometric means of VL data between days 30 and 90) for the DNA/Ad5 Mamu-A*01(+) group (GM of 1.2×10^4 copies/ml) were also 15-fold lower (95% CI of 2.2- to 100-fold) than those of the nonvaccine Mamu-A*01(+) control cohort (1.8×10^5 copies/ml). During the chronic stage, the VL levels rose in three of five DNA/Ad5 Mamu-A*01(+) animals. As a result, the differences in chronic VL (measured as the geometric means of VL between days 250 and 360) between the DNA/Ad5 and nonvaccine cohort became statistically insignificant. The differences in the mean early postacute or chronic VL between the vaccine and nonvaccine Mamu-A*01(-) cohorts were less than threefold and statistically were not meaningful. 99X032 was the only vaccinated animal that was able to control viremia to assay baseline levels starting at 4 months after challenge. The circulating CD4⁺ cell levels in the animals showed slow progressive declines throughout the course of the study (data not shown).

Certain major histocompatibility complex alleles, such as Mamu-B*17 and Mamu-A*01, have been associated with slow disease progression in macaques (22). There are six Mamu-B*17 monkeys in the study, one in each vaccine group (99C005, 99X021, and 99C230) and in the Mamu-A*01(+) control cohort (99C038) and two in Mamu-A*01(-) control group (99X033 and 99C051). Three of these did well against the SIV challenge. It should be noted that exclusion of the six animals from the analyses did not alter the statistical significance of the intercohort differences.

Postchallenge immune responses. Anamnestic Gag-specific T-cell responses were detected by CM9 tetramer staining (Fig. 3) and ELISPOT assay with the complete peptide pool (Fig. 2). CM9-specific T-cell levels for the Mamu-A*01(+) monkeys peaked between days 14 to 17; the geometric means of the peak CM9(+) cell levels for the DNA/Ad5, Ad5/Ad5, and control cohorts were 30.9% (95% CI of 19.5 to 49.1%), 19.7% (95% CI of 10.3 to 37.6%) and 1.7% (95% CI of 0.6 to 4.9%), respectively. At 25 days postchallenge, the geometric mean ELISPOT responses against the Gag peptide pool for the Mamu-A*01(-) DNA/Ad5 and control groups were 1,913 (95% CI of 792 to 4,621) and 14 (95% CI of 9 to 22) SFC/10⁶ PBMCs, respectively.

Furthermore, in the vaccinated Mamu-A*01(+) groups, the CM9-specific T-cell levels at 24 days postchallenge were negatively correlated with peak and early set-point viral loads (see Table 2), while in the Mamu-A*01(+) control group, CM9-specific T-cell levels at the same time point were positively correlated, though weakly, to the peak and early set-point viral loads. Thus, it appears that in naïve animals, specific T-cell responses are primarily driven by the high antigen load, while in vaccinated animals strong anamnestic responses translate to lower viral loads.

The phenotypes of the CM9-positive T cells in all Mamu-A*01(+) macaques were also monitored after the challenge. In every case, there was an initial rise in the fraction of tetramer-positive T cells with memory phenotype (CD45A⁻ CD27⁺ CD28⁺) peaking at the second week postchallenge (40 to 60%) (data not shown). In most animals, this subpopulation declined within the first 100 days to <10%, whereas the acute, expanding population increased to >80% of the total CM9-positive cells. The only exceptions were the two best control-

lers, 99C005 and 99C038, in which the memory pool remained above 25%. This redistribution between acute memory populations had been reported previously in HIV-infected individuals (31) and is consistent with the effect of immense antigen load from high levels of viral replication on blocking T-cell maturation to the memory status.

Responses to nonvaccine antigens such as tat, nef, rev, pol, and env were detectable as early as day 25 and are discussed in greater detail in the accompanying report (18).

Serum neutralization of SIVmac239 was determined in vitro using CEMX174 as substrate. Relatively weak neutralization titers (10 to 80) were detected in all three Mamu-A*01(+) and Mamu-A*01(-) vaccine groups as early as day 24 (data not shown). The difference in responses between any pair of vaccine groups at day 24 was not statistically significant. In comparison, detectable titers were observed no earlier than day 136 postchallenge in only four Mamu-A*01(+) and two Mamu-A*01(-) control animals.

Dynamic changes in viral load in the lymphoid tissue (LT) compartment. LT is the major reservoir for HIV-1 and SIV replication in vivo (24, 34, 35). To evaluate the efficacy of vaccine candidates in the LT compartment, lymph node (LN) biopsy samples collected at 45 and 190 days after SIV challenge were analyzed by ISH for cells with detectable SIV RNA and viral deposition on follicular dendritic cells (FDCs). At day 45, the frequency of SIV RNA(+) cells in DNA/Ad5 Mamu-A*01(+) animals was 5.3-fold (95% CI of 1.4 to 20) and 11-fold (95% CI of 1.7 to 68) lower than in Ad5/Ad5 Mamu-A*01(+) and Mamu-A*01(+) naïve control cohorts, respectively (Table 1 and Fig. 5). At the same time point, the average frequency of SIV RNA(+) cells was about twofold lower (though not statistically significant) in the DNA/Ad5 Mamu-A*01(-) group than in the control Mamu-A*01(-) group. The average frequency of SIV RNA(+) cells increased significantly in all five groups at day 190. However, the frequency of SIV RNA(+) cells remained lowest in DNA/Ad5 Mamu-A*01(+) animals (Table 1).

FDC-associated viral load is the major portion of total viral burden in HIV-1 or SIV infection (30). Using quantitative image analysis at day 45, the levels of FDC-associated viral load trended lower for both DNA/Ad5 Mamu-A*01(+) animals and DNA/Ad5 Mamu-A*01(-) animals relative to the respective control cohorts (Table 1). Similarly, the levels of FDC-associated viral load increased significantly over time in all five groups. However, the averaged level of FDC-associated viral load remained lowest for the DNA/Ad5 Mamu-A*01(+) group. Taken together, DNA/Ad5 vaccination effectively reduced the levels of set-point viral load in LN not only for Mamu-A*01(+) animals but also for Mamu-A*01(-) animals. However, continued control of viral replication in LN compartments was only evident in Mamu-A*01(+) animals at 190 days after challenge.

Correlates of vaccine efficacy. All correlation analyses were conducted using a nonparametric Spearman's ranking approach, because the exact mathematical relationships between most immunological and/or virological pairs are unknown. The observation that the DNA/Ad5 Mamu-A*01(+) animals exhibited significantly better control compared to the similarly vaccinated Mamu-A*01(-) animals implies a strong immune pressure exerted by epitopes bound by Mamu-A*01 major

TABLE 1. VLs in LT biopsy of all vaccine and control animals

Group	Animal identity no.	Frequency of SIV RNA ⁺ cells per mm ² tissue section		FDC-associated silver grain counts per mm ² tissue section	
		Day 45	Day 190	Day 45	Day 190
Mamu-A*01(+) DNA-Ad5	CC6V	0.28	2	190	34233
	99C005	0.07	0.06	296	1
	99C010	0.03	1.3	214	3927
	99C013	0.03	3.1	331	3229
	99C014	0.17	0.28	51	3341
GM		0.08	0.67	182	1077
Ad5-Ad5	99C093	0.5	0.44	4830	2043
	AW8K	0.53	0.39	2016	3077
	99C157	1.03	7.03	2811	14548
	99C230	0.12	3.02	1484	4994
	99C107	0.39	1.28	28	4552
GM		0.42	1.36	1023	4609
None	99C031	0.18	1.27	4415	5311
	99C038	0.22	0.22	24	1845
	99C066	1.18	5.41	2870	53202
	99C052	1.47	4.85	1064	6183
	99C129	6.35	1.5	20966	6836
GM		0.85	1.62	1472	7389
Mamu-A*01(-) DNA-Ad5	99X021	1.9	1.69	2573	6758
	99X022	2.22	14.4	188	52429
	99X026	2.21	2.2	488	3388
	99X029	1.03	9.8	761	32445
	99X032	0.06	0.02	60	90
GM		0.9	1.6	404	5116
None	99X033	0.66	10.2	2733	30925
	99X040	7.91	17.08	4655	21538
	99C051	0.49	0.11	1637	92
	99C090	12.39	51.82	2619	3013
	A0X001	0.36	0.35	1440	2873
GM		1.63	3.22	2393	3507

histocompatibility complex I molecules, which include the immunodominant CM9 epitope.

For the two vaccinated Mamu-A*01(+) cohorts, immune measurements such as the levels of CM9 tetramer staining 2 weeks after Ad5 boost or at the time of challenge showed a strong negative correlation with the peak plasma VL and lymphoid mononuclear cell-associated virus levels on an animal-to-animal basis (Table 2, Fig. 6A). The early-set-point VLs negatively correlated with the levels of CM9 tetramer staining 2 weeks after Ad5 boost and at the time of challenge, but it was not statistically significant for the latter (Fig. 6A). Negative correlations were also established with the peak postboost or time-of-challenge levels of IFN- γ -secreting T cells measured against the entire Gag peptide pool, consistent with the observation that the Gag-specific T-cell responses in the Mamu-A*01(+) monkeys were dominated by CM9-specific CD8⁺ T cells (Table 2). The levels of

IFN- γ -secreting T cells showed meaningful negative correlation with lymphoid FDC-associated VL at day 45. The prechallenge immune measurements remained negatively correlated with the chronic VL levels; however, unlike those for both peak and set-point VL, all these correlations were no longer statistically meaningful.

No correlations between vaccine-induced immunity and virological outcome (plasma peak, set-point, and chronic VLs) could be established in the Mamu-A*01(-) monkeys. 99X032 [Mamu-A*02(+), Mamu-A*08(+), Mamu-B*17(-)] exhibited the best control, yet this vaccine control had the weakest overall immune response. While a trend towards lower FDC-associated virus levels (day 45) was observed in the vaccinated MamuA*01(-) cohort compared to the control group, no correlation between levels of prechallenge immune responses and the FDC-associated virus levels for the vaccine cohort could be established on an animal-to-animal basis.

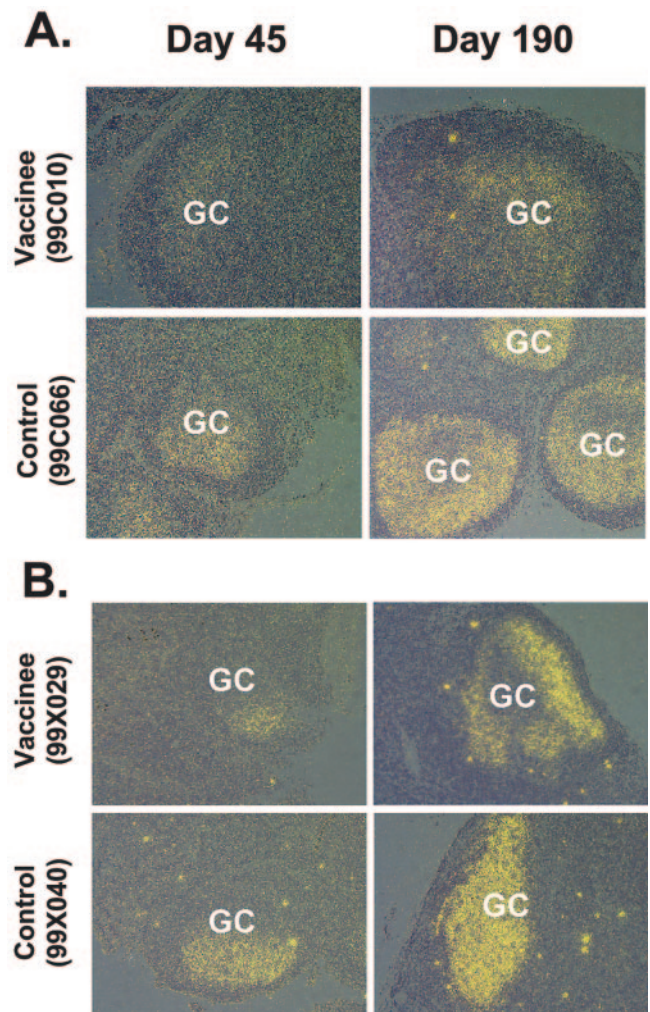


FIG. 5. In situ hybridization of SIV RNA in LN. The frequency of vRNA(+) cells and the amount of vRNA deposited on the FDC network in the germinal centers (GC) are shown for four representative monkeys, 99C010 and 99C066 (Mamu-A*01⁺) as well as 99X029 and 99X040 (Mamu-A*01⁻), at days 45 and 190 postchallenge.

TABLE 2. Rank correlations between pre- and postchallenge immune predictor variables and VLs for the 10 vaccinated Mamu-A*01(+) macaques^a

Immune parameters	Peak VL	GM VL (day 30–90)	GM VL (day 90–250)	GM VL (day 250–350)	MNC VL (day 45)	FDC VL (day 45)
CM9 tet (wk 26)	<i>-0.82, 0.002</i>	<i>-0.72, 0.009</i>	-0.31, 0.20	-0.43, 0.11	<i>-0.66, 0.020</i>	-0.21, 0.28
CM9 tet (wk 36)	<i>-0.78, 0.004</i>	-0.54, 0.053	-0.27, 0.22	-0.18, 0.31	<i>-0.66, 0.018</i>	-0.28, 0.21
CM9 tet (day 24 PC)	<i>-0.60, 0.044</i>	<i>-0.65, 0.028</i>	<i>-0.58, 0.049</i>	-0.53, 0.069	<i>-0.85, 0.002</i>	-0.28, 0.23
SFC/10 ⁶ PBMC, gag (wk 28)	<i>-0.68, 0.015</i>	<i>-0.66, 0.020</i>	-0.39, 0.13	-0.42, 0.12	<i>-0.72, 0.010</i>	<i>-0.62, 0.026</i>
SFC/10 ⁶ PBMC, gag (wk 36)	<i>-0.70, 0.013</i>	<i>-0.71, 0.010</i>	<i>-0.56, 0.045</i>	-0.43, 0.11	<i>-0.80, 0.003</i>	<i>-0.55, 0.049</i>

^a Input immune variables are CM9-specific T-cell levels (CM9 tet) measured at different time points, such as week 26 (2 weeks postboost), week 36 (at challenge), and 24 days postchallenge (PC), and ELISPOT responses against the Gag peptide pool (SFC/10⁶ PBMC, gag) measured at week 28 (4 weeks postboost) and week 36. Response variables include peak VL calculated as the maximum VL value over the first month postchallenge; geometric means of recorded VLs over the indicated time period postchallenge (in days); and VL values associated with lymph tissues, namely, those found with follicular dendritic cells (FDC) and mononuclear cells (MNC). Each entry contains the Spearman's Rho correlation coefficient followed by the one-tailed P value. Correlations with P values of less than 0.05 are highlighted in italics.

We previously reported the efficacy of several gag-expressing vaccine vectors in an SHIV89.6P challenge model, in which attenuation of VL and protection against CD4 lymphopenia were achieved (28). It is interesting to note that equivalent parameters such as the peak postboost and time-of-challenge CM9 staining highly determined the outcome of infection with either virus (Fig. 6B). The difference in the effect on both viruses lies in the degree of attenuation induced by the vaccine. Specifically, much higher immunity (as measured by CM9 tetramer staining) was required for a vaccine to have an impact on SIV replication than on SHIV89.6P.

Additional evidence suggesting the role of the CM9-directed responses in immune control arises from the changes in levels of CM9-specific T cells during the postacute phase (Fig. 3). A decline in CM9-positive T-cell level during the chronic phase was previously associated with occurrence of escape mutants (4, 9) due to immune pressure exerted by these T cells. Only one of four monkeys in the DNA/Ad5 cohort for which the CM9-positive lymphocyte levels were closely monitored had a dramatic drop in CM9 levels, compared to 4 out of 5 and 3 out

of 5 animals in the Ad5/Ad5 and control groups, respectively. While viruses with CM9-localized mutations were observed in these animals, they do not fully account for the viral rebounds observed in this study (18). It is important to realize that epitopes other than CM9 also contribute to the dynamics of the control of SIVmac239 infection (18). An understanding of these factors should enhance our ability to establish strong correlates of protection in this animal model.

On an animal-to-animal basis, no significant correlation was observed between VL (peak or set-point) and the neutralization titers at day 24 either for all 15 vaccinees or for all 10 Mamu-A*01(+) vaccinees. This suggests that virus-specific neutralizing antibodies do not notably influence differences in the course of viral infection among the vaccinees.

DISCUSSION

We had previously reported the efficacy of immunization with DNA and Ad5 vectors expressing gag in attenuating virus load and associated progression to clinical disease in monkeys challenged with SHIV89.6P (28). In this latter study, the Ad5 vaccine vector mediated a noted attenuating effect. So as to further extend these observations, we subsequently conducted the study reported here in which DNA and Ad5 gag-expressing vaccine vectors were used to immunize rhesus macaques which were then challenged intrarectally with SIVmac239. Unlike SHIV89.6P, SIVmac239 has been reported to be largely refractory to many of the vaccine modalities that are currently undergoing development (13, 32). Our observations confirm this; nonetheless, a distinct attenuation of the virus replication was seen with regard to early virus replication in one cohort of immunized animals compared to that of controls. This cohort had been immunized with a DNA vector prime followed by an Ad5 boost and, due to its Mamu A*01-positive nature, exhibited a strongly dominant CD8⁺ T-cell response directed against the viral Gag antigen. The animal cohorts that had received a slightly less potent immunization series (Ad5 for both priming and boosting) or that exhibited a less dominant response (Mamu A*01-negative animals) did not exhibit an attenuation of virus load following challenge. The association of viral control with a defined major histocompatibility complex allele (Mamu-A*01) strongly supports that vaccine-induced cytotoxic T lymphocytes can negatively affect replication of a difficult immunodeficiency virus in macaques. These findings also suggests that in humans, host-dependent factors such

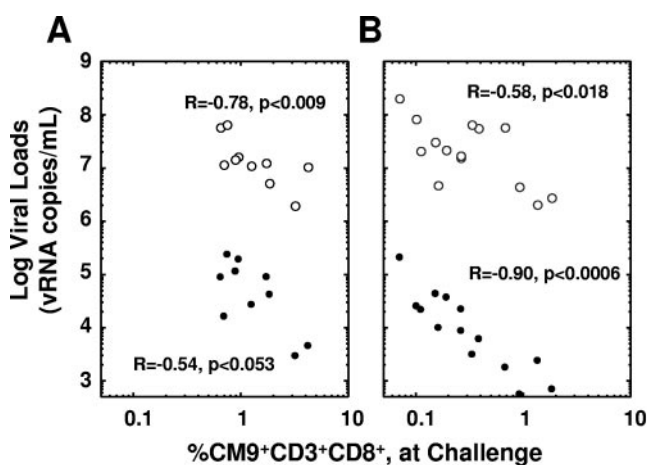


FIG. 6. Association of reduced peak VL (open circles) and postacute VL (filled circles) with CM9-specific T-cell levels at the time of challenge with either SIVmac239 (A) or SHIV89.6P (B) (28). The postacute viral burden for each animal was calculated as the geometric means of the VL from months 2 and 3. Analyses of correlation between the VL and CM9 levels were conducted using Spearman's rho. The correlation coefficients (R) and P values (one-tailed) for each group are shown.

as HLA genes will clearly contribute to the variability in efficacy of an HIV vaccine (15, 19, 21, 23, 35). The HLA diversity in a patient population must be adequately addressed during the course of clinical trials in order to comprehend the scope of the effectiveness of these vaccines.

Interestingly, the more profound antiviral effects seen in the earlier SHIV89.6P study and the more modest effects observed in the present SIVmac239 study both appear to correlate with the levels of vaccine-elicited specific T-cell responses. This suggests that the differences between the two studies primarily represent differences in the degree of the vaccine-mediated effects with regard to two challenge viruses that present with notably diverse patterns of virus replication and associated pathology. Higher levels of vaccine-induced immunity are required to have a tangible impact on SIV replication than on SHIV89.6P. Furthermore, immune control was more prolonged and pronounced against SHIV89.6P. Despite the evidence of control during the first 100 days of SIV infection, the levels of viral replication remained higher than those observed with SHIV89.6P control; these ultimately could lead to the emergence of escape mutants and/or continued destruction of the lymphoid architecture, resulting in a weakened immune system.

Regardless of which trend in immune control, that associated with an SHIV challenge or that associated with an SIV challenge, will closely approximate the potential effects of a prophylactic vaccine on HIV-1 infection, the answer will have to await the outcome of long-term human efficacy trials conducted using vaccines such as those evaluated here. Importantly, however, our observations support the perspective that such human trials should be optimally performed with vaccine modalities that are capable of eliciting very robust levels of virus-specific cellular immunity.

ACKNOWLEDGMENTS

We thank Ron Desrosiers for the gift of the SIVmac239 virus stock; we also acknowledge Karen Wright, Larry Handt, Jane Fontenot, and Robert Druilhet for assistance with the animal experiments.

REFERENCES

- Allen, T. M., L. Mortara, B. R. Mothe, M. Liebl, P. C. Jing, B. Calore, M. Piekarczyk, R. Ruddersdorf, D. H. O'Connor, X. Wang, C. X. Wang, D. B. Allison, J. D. Altman, A. Sette, R. C. Desrosiers, G. Sutter, and D. I. Watkins. 2002. Tat-vaccinated macaques do not control simian immunodeficiency virus SIVmac239 replication. *J. Virol.* **76**:4108–4112.
- Amara, R. R., J. M. Smith, S. I. Staprans, D. C. Montefiori, F. Villinger, J. D. Altman, S. P. O'Neil, N. L. Kozyr, Y. Xu, L. S. Wyatt, P. L. Earle, J. G. Herndon, H. M. McClure, B. Moss, and H. L. Robinson. 2002. Critical role for Env as well as Gag-Pol in control of a simian-human immunodeficiency virus 89.6P challenge by a DNA prime/recombinant modified vaccinia virus Ankara vaccine. *J. Virol.* **76**:6138–6146.
- Barouch, D., S. Santra, M. J. Kuroda, J. E. Schmitz, R. Plishka, A. Buckler-White, A. E. Gaitan, R. Zin, J. H. Nam, L. S. Wyatt, M. A. Lifton, C. E. Nickerson, B. Moss, D. C. Montefiori, V. M. Hirsch, and N. L. Letvin. 2001. Reduction of simian-human immunodeficiency virus 89.6P viremia in rhesus monkeys by recombinant modified vaccinia virus Ankara vaccination. *J. Virol.* **75**:5151–5158.
- Barouch, D. H., J. Kunstman, M. J. Kuroda, J. E. Schmitz, S. Santra, F. W. Peyerl, G. R. Krivulka, K. Beaudry, M. A. Lifton, D. A. Gorgone, D. C. Montefiori, M. G. Lewis, S. M. Wolinsky, and N. L. Letvin. 2002. Eventual AIDS vaccine failure in a rhesus monkey by viral escape from cytotoxic T lymphocytes. *Nature* **415**:335–339.
- Caley, I. J., M. R. Betts, D. M. Irlbeck, N. L. Davis, R. Swanstrom, J. A. Frelinger, and R. E. Johnston. 1997. Humoral, mucosal, and cellular immunity in response to a human immunodeficiency virus type 1 immunogen expressed by a Venezuelan equine encephalitis virus vaccine vector. *J. Virol.* **71**:3031–3038.
- Casimiro, D. R., L. Chen, T. Fu, R. K. Evans, M. J. Caulfield, M. Davies, A. Tang, M. Chen, L. Huang, V. Harris, D. C. Freed, K. A. Wilson, S. Dubey, D. Zhu, D. Nawrocki, H. Mach, R. Troutman, L. Isopi, D. Williams, W. Hurni, Z. Xu, J. G. Smith, S. Wang, X. Liu, L. Guan, R. Long, W. Triglona, G. J. Heidecker, H. C. Perry, N. Persaud, T. J. Toner, Q. Su, X. Liang, R. Youil, M. Chastain, A. J. Bett, D. B. Volkin, E. A. Emini, and J. W. Shiver. 2003. Comparative immunogenicity in rhesus monkeys of DNA plasmid, recombinant vaccinia and replication-defective adenoviral vectors expressing a human immunodeficiency virus type 1 gag gene. *J. Virol.* **77**:6305–6313.
- Davis, N. L., A. West, E. Reap, G. MacDonald, M. Collier, S. Dryga, M. Maughan, M. Connell, C. Walker, K. McGrath, C. Cecil, L. H. Ping, J. Frelinger, R. Olmsted, P. Keith, R. Swanstrom, C. Williamson, P. Johnson, D. Montefiori, and R. E. Johnston. 2002. Alphavirus replicon particles as candidate HIV vaccines. *IUBMB-LIFE* **53**:209–211.
- Evans, T. G., M. C. Keefer, K. J. Weinhold, M. Wolff, D. Montefiori, G. J. Gorse, B. S. Graham, M. J. McElrath, M. L. Clements-Mann, M. J. Mulligan, P. Fast, M. C. Walker, J. L. Excler, A. M. Duliege, and J. Tartaglia. 1999. A canarypox vaccine expressing multiple human immunodeficiency virus type 1 genes given alone or with rgp120 elicits broad and durable CD8⁺ cytotoxic T lymphocyte responses in seronegative volunteers. *J. Infect. Dis.* **180**:290–298.
- Friedrich, T. C., E. J. Dodds, L. J. Yant, L. Vojnov, R. Ruddersdorf, C. Cullen, D. T. Evans, R. C. Desrosiers, B. R. Mothe, J. Sidney, A. Sette, K. Kunstman, S. Wolinsky, M. Piatak, J. Lifson, A. L. Hughes, N. Wilson, D. H. O'Connor, and D. I. Watkins. 2004. Reversion of CTL escape-variant immunodeficiency viruses in vivo. *Nat. Med.* **10**:275–281.
- Hanke, T., R. V. Samuel, T. J. Blanchard, V. C. Neumann, T. M. Allen, J. E. Boyson, S. S. Sharpe, N. Cook, G. L. Smith, D. I. Watkins, M. P. Cranage, and A. J. McMichael. 1999. Effective induction of simian immunodeficiency virus-specific cytotoxic T lymphocytes in macaques by using a multi-epitope gene and DNA prime-modified vaccinia virus Ankara boost vaccination regimen. *J. Virol.* **73**:7524–7532.
- Hel, Z., J. Nacsa, E. Tryniszewska, W. P. Tsai, R. W. Parks, D. C. Montefiori, B. K. Felber, J. Tartaglia, G. N. Pavlakis, and G. Franchini. 2002. Containment of simian immunodeficiency virus infection in vaccinated macaques: correlation with the magnitude of virus-specific pre- and postchallenge CD4(+) and CD8(+) T cell responses. *J. Immunol.* **169**:4778–4787.
- Hollander, M., and D. Wolfe. 1999. Nonparametric statistical methods, 2nd ed. Wiley-Interscience, New York, N.Y.
- Horton, H., T. U. Vogel, D. K. Carter, K. Vielhuber, D. H. Fuller, T. Shipley, J. T. Fuller, K. J. Kunstman, G. Sutter, D. C. Montefiori, V. Erffe, R. C. Desrosiers, N. Wilson, L. J. Picker, S. M. Wolinsky, C. Wang, D. B. Allison, and D. I. Watkins. 2002. Immunization of rhesus macaques with a DNA prime/modified vaccinia virus Ankara boost regimen induces broad simian immunodeficiency virus (SIV)-specific T-cell responses and reduces initial viral replication but does not prevent disease progression following challenge with pathogenic SIVmac239. *J. Virol.* **76**:7187–7202.
- Jin, X., D. E. Bauer, S. E. Tuttleton, S. Lewin, A. Gettje, J. Blanchard, C. E. Irwin, J. T. Safrit, J. Mittler, L. Weinberger, L. G. Kostrikis, L. Q. Zhang, A. S. Perelson, and D. D. Ho. 1999. Dramatic rise in plasma viremia after CD8(+) T cell depletion in simian immunodeficiency virus-infected macaques. *J. Exp. Med.* **189**:991–998.
- Kaslow, R. C., M. Carrington, R. Apple, L. Park, A. Munoz, A. J. Saah, J. J. Goedert, C. Winkler, S. J. O'Brien, C. Rinaldo, R. Detels, W. Blattner, J. Phair, H. Ehrlich, and D. L. Mann. 1996. Influence of combinations of human major histocompatibility complex genes on the course of HIV-1 infection. *Nat. Med.* **2**:405–411.
- Knapp, L. A., E. Lehmann, M. S. Piekarczyk, J. A. Urvater, and D. I. Watkins. 1997. A high frequency of Mamu-A*01 in the rhesus macaque detected by polymerase chain reaction with sequence-specific primers and direct sequencing. *Tissue Antigens* **50**:657–661.
- Koup, R. A., J. T. Safrit, Y. Cao, C. A. Andrews, G. McLeod, W. Borkowsky, C. Farthing, and D. D. Ho. 1994. Temporal association of cellular immune responses with the initial control of viremia in primary human immunodeficiency virus type 1 syndrome. *J. Virol.* **68**:4650–4655.
- McDermott, A. B., D. H. O'Connor, S. Fuenger, S. Piaskowski, S. Martin, J. Loffredo, M. Reynolds, J. Reed, J. Furlott, T. Jacoby, C. Riek, E. Dodds, K. Krebs, M. Davies, W. Schleif, D. R. Casimiro, J. W. Shiver, and D. I. Watkins. 2005. Cytotoxic T-lymphocyte escape does not always explain the transient control of simian immunodeficiency virus SIVmac239 viremia in adenovirus-boosted and DNA-primed boosted Mamu-A*01-positive rhesus macaques. *J. Virol.* **79**:15556–15566.
- Migueles, S. A., M. S. Sabbaghian, W. L. Shupert, M. P. Bettinotti, F. M. Marincola, L. Martino, C. W. Hallahan, S. M. Selig, D. Schwartz, J. Sullivan, and M. Connors. 2000. HLA B*5701 is highly associated with restriction of virus replication in a subgroup of HIV-infected long term nonprogressors. *Proc. Natl. Acad. Sci. USA* **97**:2709–2714.
- Montefiori, D. C., T. W. Baba, A. Li, M. Bilska, and R. M. Ruprecht. 1996. Neutralizing and infection-enhancing antibody responses do not correlate with the differential pathogenicity of SIVmac239delta3 in adult and infant rhesus monkeys. *J. Immunol.* **157**:5528–5535.
- Mothe, B. R., J. Weinfurter, C. X. Wang, W. Rehrauer, N. Wilson, T. M.

- Allen, D. B. Allison, and D. I. Watkins. 2003. Expression of the major histocompatibility complex class I molecule Mamu-A*01 is associated with control of simian immunodeficiency virus SIV239 replication. *J. Virol.* 77:2736–2740.
22. O'Connor, D. H., B. R. Mothe, J. T. Weinfurter, S. Fuenger, W. M. Rehrauer, P. Jing, R. R. Rudersdorf, M. E. Liebl, K. Krebs, J. Vasquez, E. Dodds, J. Loffredo, S. Martin, A. B. McDermott, T. M. Allen, C. Wang, G. G. Doxiadis, D. C. Montefiori, A. Hughes, D. R. Burton, D. B. Allison, S. M. Wolinsky, R. Bontrop, L. J. Picker, and D. I. Watkins. 2003. Major histocompatibility complex class I alleles associated with slow simian immunodeficiency virus disease progression bind epitopes recognized by dominant acute-phase cytotoxic-T-lymphocyte responses. *J. Virol.* 77:9029–9040.
 23. Pal, R., D. Venzon, N. L. Letvin, S. Santra, D. C. Montefiori, N. R. Miller, E. Tryniszewska, M. G. Lewis, T. C. VanCott, V. Hirsch, R. Woodward, A. Gibson, M. Grace, E. Dobratz, P. D. Markham, Z. Hel, J. Nacs, M. Klein, J. Tartaglia, and G. Franchini. 2002. ALVAC-SIV-gag-pol-env-based vaccination and macaque major histocompatibility complex class I (A*01) delay simian immunodeficiency virus SIVmac-induced immunodeficiency. *J. Virol.* 76:292–302.
 24. Pantaleo, G., C. Graziosi, J. F. Demarest, L. Butini, M. Montroni, C. H. Fox, J. M. Orenstein, D. P. Kotler, and A. S. Fauci. 1993. HIV infection is active and progressive in lymphoid tissue during the clinically latent stage of disease. *Nature* 362:355–358.
 25. Schmitz, J. E., M. J. Kuroda, S. Santra, V. G. Sasseville, M. A. Simon, M. A. Lifton, P. Racz, K. Tenner Racz, M. Dalesandro, B. J. Scallon, J. Ghayeb, M. A. Forman, D. C. Montefiori, E. P. Rieber, N. L. Letvin, and K. A. Reimann. 1999. Control of viremia in simian immunodeficiency virus infection by CD8⁺ lymphocytes. *Science* 283:857–860.
 26. Seaman, M. S., L. Xu, K. Beaudry, K. L. Martin, M. H. Beddall, A. Miura, A. Sambor, N. K. Chakrabarti, Y. Huang, R. Bailer, R. A. Koup, J. R. Mascola, G. J. Nabel, and N. L. Letvin. 2005. Multiclad human immunodeficiency virus type 1 envelope immunogens elicit broad cellular and humoral immunity in rhesus monkeys. *J. Virol.* 79:2956–2963.
 27. Seth, A., I. Ourmanov, J. E. Schmitz, M. J. Kuroda, M. A. Lifton, C. E. Nickerson, L. Wyatt, M. Carroll, B. Moss, D. Venzon, N. L. Letvin, and V. M. Hirsch. 2000. Immunization with a modified vaccinia virus expressing simian immunodeficiency virus (SIV) Gag-Pol primes for an anamnestic Gag-specific cytotoxic T-lymphocyte response and is associated with reduction of viremia after SIV challenge. *J. Virol.* 74:2502–2509.
 28. Shiver, J. W., T.-M. Fu, L. Chen, D. R. Casimiro, M. Davies, R. K. Evans, Z.-Q. Zhang, A. J. Simon, W. L. Trigona, S. A. Dubey, L. Huang, V. A. Harris, R. S. Long, X. Liang, L. Handt, W. A. Schleif, L. Zhu, D. C. Freed, N. V. Persaud, L. Guan, K. S. Punt, A. Tang, M. Chen, K. A. Wilson, K. B. Collins, G. J. Heidecker, V. R. Fernandez, H. C. Perry, J. G. Joyce, K. M. Grimm, J. C. Cook, P. M. Keller, D. S. Kresock, H. Mach, R. D. Troutman, L. A. Isopi, D. M. Williams, Z. Xu, K. E. Bohannon, D. B. Volkin, D. C. Montefiori, A. Miura, G. R. Krivulka, M. A. Lifton, M. J. Kuroda, J. E. Schmitz, N. L. Letvin, M. J. Caulfield, A. J. Bett, R. Youil, D. C. Kaslow, and E. A. Emini. 2002. Replication-incompetent adenoviral vaccine vector elicits effective anti-immunodeficiency-virus immunity. *Nature* 415:331–335.
 29. Shiver, J. W., H. C. Perry, M. E. Davies, and M. A. Liu. 1995. Immune responses to HIV gp120 elicited by DNA vaccination, p. 95. *In* R. M. Chanock, F. Brown, H. S. Ginsberg, and E. Norrby (ed.), *Vaccines 95*. Cold Spring Harbor Laboratory Press, Cold Spring Harbor, N.Y.
 30. Tenner Racz, K., and P. Racz. 1995. Follicular dendritic cells initiate and maintain infection of the germinal centers by human immunodeficiency virus. *Curr. Top. Microbiol. Immunol.* 201:141–159.
 31. Tussey, L. G., U. S. Nair, M. Bachinsky, B. H. Edwards, J. Bakari, K. Grimm, J. Joyce, R. Vessey, R. Steigbigel, M. N. Robertson, J. W. Shiver, and P. A. Goepfert. 2003. Antigen burden is major determinant of human immunodeficiency virus-specific CD8⁺ T cell maturation state: potential implications for therapeutic immunization. *J. Infect. Dis.* 187:364–374.
 32. Vogel, T. U., M. R. Reynolds, D. H. Fuller, K. Vielhuber, T. Shipley, J. T. Fuller, K. J. Kunstman, G. Sutter, M. L. Marthas, V. Erfle, S. M. Wolinsky, C. X. Wang, D. B. Allison, E. W. Rud, N. Wilson, D. Montefiori, J. D. Altman, and D. I. Watkins. 2003. Multispecific vaccine-induced mucosal cytotoxic T lymphocytes reduce acute-phase viral replication but fail in long-term control of simian immunodeficiency virus SIVmac239. *J. Virol.* 77:13348–13360.
 33. Xin, K. Q., M. Urabe, J. Yang, K. Nomiya, H. Mizukami, K. Hamajima, H. Nomiya, T. Saito, M. Imai, J. Monahan, K. Okuda, K. Ozawa, and K. Okuda. 2001. A novel recombinant adeno-associated virus vaccine induces a long-term humoral immune response to human immunodeficiency virus. *Hum. Gene Ther.* 12:1047–1061.
 34. Zhang, Z. Q., T. Schuler, M. Zupancic, S. Wietgreffe, K. A. Staskus, K. A. Reimann, T. A. Reinhart, M. Rogan, W. Cavert, C. J. Miller, R. S. Veazey, D. Notermans, S. Little, S. A. Danner, D. D. Richman, D. Havlir, J. Wong, H. L. Jordan, T. W. Schacker, P. Racz, K. Tenner-Racz, N. L. Letvin, S. Wolinsky, and A. T. Haase. 1999. Sexual transmission and propagation of SIV and HIV in resting and activated CD4(+) T cells. *Science* 286:1353–1357.
 35. Zhang, Z. Q., T. Fu, D. R. Casimiro, M. Davies, X. Liang, W. A. Schleif, L. Handt, L. Tussey, M. Chen, A. Tang, K. A. Wilson, W. L. Trigona, D. C. Freed, C. Y. Tan, M. Horton, E. A. Emini, and J. W. Shiver. 2002. Mamu-A*01 allele-mediated attenuation of disease progression in simian-human immunodeficiency virus infection. *J. Virol.* 76:12845–12854.